Introducing Glory: A Novel Strategy for an Omnidirectional Spherical Rolling Robot

Amir Homayoun Javadi A.
Azad University of Qazvin,
Electronics and Computer Engineering Department,
Iran
e-mail: javadi@anoise.com

Puyan Mojabi
Iran University of Science and Technology,
Electrical and Computer Engineering Department,
Iran
e-mail: mojabi@anoise.com

This paper describes a prototype and analytical studies of a spherical rolling robot, a new design of an omnidirectional robot system. The robot can arbitrarily begin to move in any direction to the target, and autonomously roll and reach any desired position. Our design has considered a spherical robot with an internal mechanism for propulsion. The propulsion mechanism will distribute weights radially along spokes fixed inside the sphere and enables the robot to accelerate, decelerate, and move with constant velocity. A mathematical model of the robot's dynamic and motion was instructed. An algorithmic motion planning is developed and, partly, pseudocode of that is presented. For a number of missions, it is shown experimentally that the model agrees well with the results. [DOI: 10.1115/1.1789542]

1 Introduction

We are in the process of developing a spherical mobile robot that has improved mobility and maneuverability than existing wheel- and track-based mobile robots. The robot, shown in Fig. 1, will have an external spherical skeleton, an internal propulsion mechanism, an interface for remote operation, and an intelligent control system that completely exploits its full range of mobility.

The spherical exoskeleton will provide the robot with maximal stability in the absence of orientation preference, and the ability to roll in all directions rather than one, as provided by the wheel. Being the outer perimeter of the robot and therefore relatively large in dimension, the external skeleton will provide the ability to roll over rough terrain with relative ease. The skeleton, through proper material selection, will circumscribe all hardware including controllers and actuators. The internal propulsion mechanism will provide the robot with rapid maneuverability by enabling it to quickly accelerate and decelerate, or move with constant velocity. The propulsion mechanism will also allow the robot to climb slopes of considerable inclination and traverse terrain with significant undulations in contrast with previous spherical robots.

The outline of the paper is as following: Section 2 presents works on omnidirectional robots with an emphasis on spherical rolling robots; Sec. 3 gives a description of the system.

Section 4 presents the mathematical model of the robot followed with trajectory planning in Sec. 5; Sec. 6 is devoted to experimental results, and concluding remarks are presented in Sec. 7.

Contributed by the Dynamic Systems, Measurement, and Control Division of THE AMERICAN SOCIETY OF MECHANICAL ENGINEERS for publication in the ASME JOURNAL OF DYNAMIC SYSTEMS, MEASUREMENT, AND CONTROL. Manuscript received by the ASME Dynamic Systems and Control Division December 3, 2003. Associate Editor: M. Goldfarb.

2 Related Work

The holonomic or nonholonomic omnidirectional mobile robots have been studied by using a variety of mechanisms [1–4]. In other words, several omnidirectional platforms have been known to be realized by developing a specialized wheel or mobile mechanism. Mobile robots of a spherical shape have been described by only a few authors. The first spherical robot was developed by Halme et al. [5]. They proposed a spherical robot with a single wheel resting on the bottom of a sphere. Bicchi et al. [6] developed a spherical vehicle consisting of a hollow sphere with a small car resting on the bottom. Ball robot designs [5,6] complicate the control problem by imposing nonholonomic constraints both inside and outside the sphere [8]. Bhattacharya et al. [7] proposed a driving mechanism that is a set of two mutually perpendicular rotors attached to the inside of the sphere. Ferriere et al. [9] developed a universal wheel to actuate a spherical ball to move the system, and in their mechanism, the actuation system is out of the sphere. It is, however, obvious that the autonomous spherical rolling robot, described in this paper, Glory, differs from the previous designs. The driving mechanism is a set of four spokes distributing weights radially along them inside the sphere, in contrast to a wheel resting at the bottom of the sphere or, two mutually perpendicular rotors attached to the inside of the sphere, in previous works. The salient features of different experimental designs of a ball robot are summarized in Fig. 2. Mukherjee et al. [8] studied the feasibility of moving a spherical robot to an arbitrary point and orientation. They had presented two strategies for reconfiguration. Glory is the only implemented spherical robot which can traverse omnidirectionaly.

3 System Description

The spherical robot (nicknamed ''Glory''), shown in Fig. 1, consists of a hollow ball rolling freely on the floor. The robot is powered autonomously; its logic is partly implemented onboard and partly in a base station, connected through a radio link.

Glory is so assembled that the whole system has geometrical symmetry. The result of this symmetry is that the center of mass of the robot, despite weights, always lies exactly at the geometric center of the sphere, above its contact point. Thus, the robot does not tend to ''tip over.'' This point is important in the development of the analytical model of robot's dynamics.

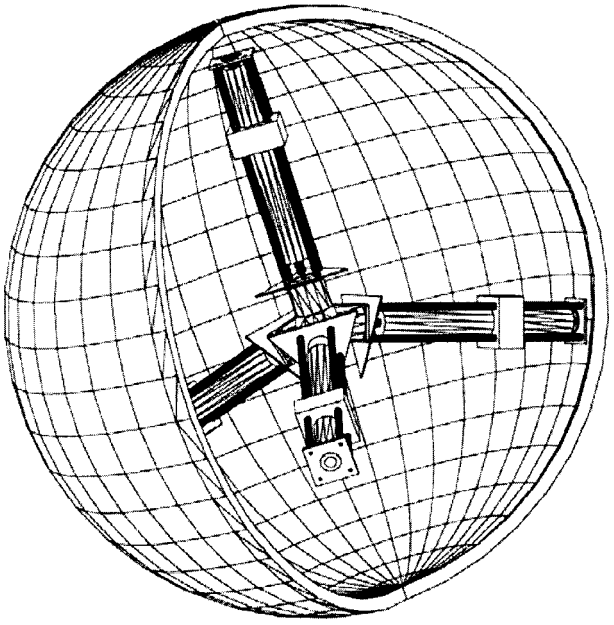

Fig. 1 Inner propulsion system showing whole the system

Halme et al., 1996	Bicchi et al., 1997	Bhattacharya and Agrawal, 2000	Javadi and Mojabi, 2002
Single Wheel	Car	Attached rotors	Fixed Internal Propulsion
1 Input	2 Inputs	2 Inputs	4 Inputs
Open-loop, no planning	Closed-loop, kinematic planning	Open-loop, dynamic planning	Open-loop, dynamic planning

Fig. 2 Comparison of spherical robots

3.1 Propulsion Mechanism. The propulsion mechanism consists of four power screwed spokes, connected in 109.47°, as shown in the Appendix, inside a tetrahedral shape, Fig. 1. There are four 1.125 kg weights placed through spokes, which are elevated upward and downward using four stepper motors, with 200 steps per revolution, connected directly to the spokes, as shown in Fig. 3.

3.2 External Camera as Feedback. Glory's outer surface is blue with two red stripes going around it. These marks are used by the camera to locate the robot from a top view. A video handy camera is mounted pointing straight down 2.6 m above the robot. The video camera takes 600 by 800 pixel color images of the moving boundaries.

3.3 Controller. The stepper circuit is driven by a square wave generated directly by a microcontroller, which is mounted on board the robot. The microcontroller receives high-level planning instructions, per step, from an remove computer via a unidirectional parallel radio link at 6200 bps. A computer using dynamic model of the robot and images from camera makes all decisions. The microcontroller, inside the robot, uses information received through radio link to carry out desired for stepper motors, and microcontroller and wireless link are just an interface between computer and motors.

4 Analytical Model

Glory is considered to be a system of three different sets of bodies:

• weights as four dynamic bodies which their distance related to the center of the sphere changes time by time;

• the spherical shell, motors, and cylindrical power screws, as static bodies which their status related to the center of the sphere does not change;

• other components, such as fasteners, which for the sake of simplicity, are neglected from the model, in contrast with other components.

An initial coordinate frame is attached to the surface and denoted as XYZ with its origin at point O_i, which O_i is the center point of the robot in the beginning of movement. The body coordinates xyz, parallel to XYZ, are attached to the sphere and have their origin at the center of the sphere O, as shown in Fig. 4.

4.1 Complete Dynamic Model and Analysis. When the complete dynamics of the weights are taken into consideration, the governing equations of motion become very complicated and pose a challenging trajectory control problem. We have adopted a Newton formulation for propulsion mechanism since the acceleration of the sphere appears explicitly in the equation. These equations have the form

$$\sum \vec{M} = \left(\sum [I] \right) \cdot \dot{\vec{\omega}} + \sum \vec{\rho}_i \times m \ddot{\vec{\rho}}, \tag{1}$$

where $(\Sigma \vec{M})$ is the moment due to the weights of the individual unbalanced masses, I is the moment of inertia of the robot and $\dot{\vec{\omega}}$ is the angular acceleration of the sphere. The vector $\vec{\rho}_i$ represents the position vector of ith weight with respect to the relative spoke. The vectors represented by $\ddot{\vec{\rho}}_i$ are equivalent to the absolute accelerations of individual weights.

In our implementation, due to the discrete nature of stepper motors, we can suppose, for each step of simulation, each weight is temporarily fixed in its position related to the center of robot. Thus, we can neglect the second term on the right-hand side of the equation in a good rate of approximation. It helps us to calculate angular acceleration.

4.2 Analysis Based on a Static Model. The static model provides a simpler solution with less computation. A static analysis only considers the moments due to the weights of the unbalanced masses and has the following form:

$$\sum \vec{M} = \left(\sum [I] \right) \cdot \dot{\vec{\omega}}. \tag{2}$$

In our algorithm, The acceleration profile is scaled at every instant to meet the physical constraints of weights, and find the instantaneous position of the masses.

4.3 Moment Vector. Moment vector can be calculated as below:

$$\vec{M} = \vec{w} \times \vec{d}, \tag{3}$$

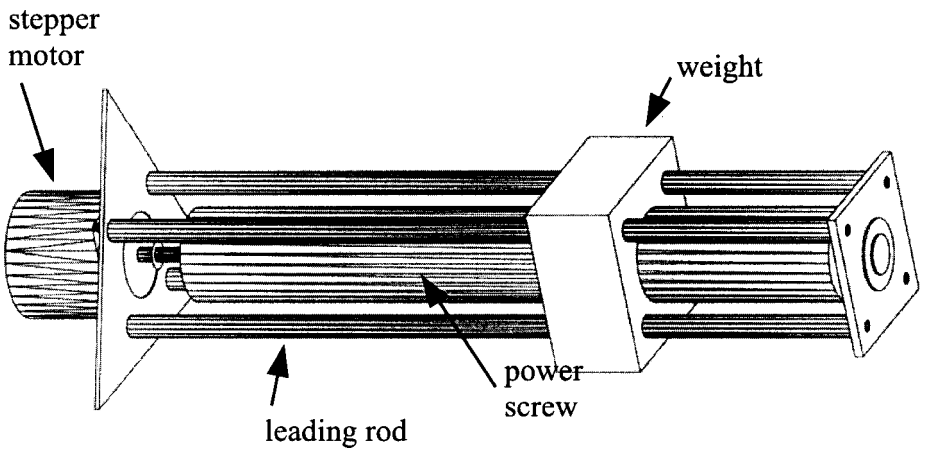

Fig. 3 A closeup of a spoke containing a stepper motor, a cylindrical screw, and a weight

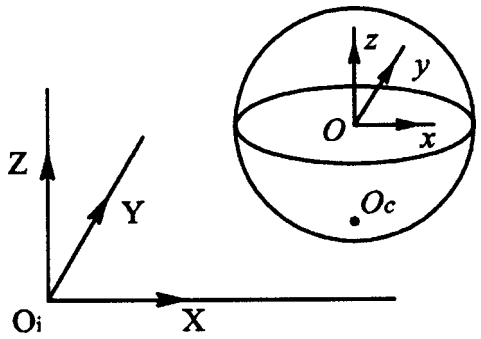

Fig. 4 A sphere rolling on a plane; $O_i(0,0,0)$, $O(x,y,0)$, $O_c(x,y,-r)$ (where r is the radius of the spherical shell)

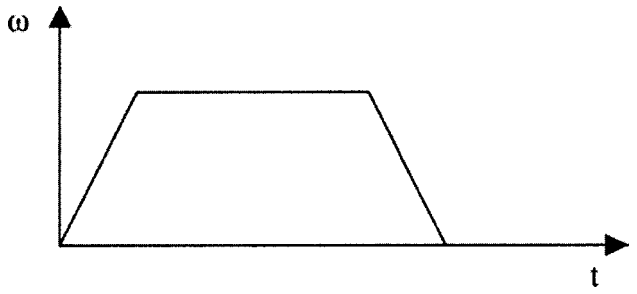

Fig. 5 Angular velocity and time diagram of robot motion, from beginning to destination

where $\vec{w}$ is the weight vector, and $\vec{d}$ is the distance vector.

Because of geometrical symmetry of other bodies, weights are the only bodies that cause moment, which their inter-relation defines the movement direction. Therefore, the resultant moment vector is as following, which is the main relation showing the direction of movement in plane:

$$\vec{M} = m^w g \begin{bmatrix} -y_1 - y_2 - y_3 - y_4 \\ x_1 + x_2 + x_3 + x_4 \\ 0 \end{bmatrix}, \tag{4}$$

where m^w is the weight of an unbalanced mass, and x_i and y_i are the position of the ith weight $(1 \leqslant i \leqslant 4)$.

4.4 Moment of Inertia. For calculating the moment of inertia we use a 3×3 matrix as below:

$$I = \begin{bmatrix} I_{xx} & I_{xy} & I_{xz} \\ I_{yx} & I_{yy} & I_{yz} \\ I_{zx} & I_{zy} & I_{zz} \end{bmatrix} \tag{5}$$

which I_{xx} and I_{xy} are as follows:

$$I_{xx} = \bar{I}_{xx} + m d_x^2, \tag{6}$$

$$I_{xy} = \bar{I}_{xy} + m d_x d_y, \tag{7}$$

and the other components of I are calculated likewise. Equations (6) and (7) are transfer-of-axis relations for transferring I from the center of mass to O. Also, in Eq. (5), due to symmetrical design of the robot $I_{ij} = I_{ji}$.

4.5 No-Slip Constraint. We assume that the robot rolls without slipping. Hence, the velocity of the contact point O_c with respect to the inertial coordinates is zero, i.e., $v_{O_c} = 0$.

4.6 Angular Momentum Conservation. Due to the symmetric design of the robot, the gravity force acts vertically through the center and the point of contact. The ground reaction force and frictional force also act through the point of contact. Hence, the sum of external moments at the point O_c is therefore zero. Hence, the rate of change of the angular momentum measured at O_c is $\dot{H}_{O_c} = 0$ [10]. Hence, the angular momentum of the robot at O_c is a conserved quantity. Furthermore, we assume that the robot starts from rest, i.e., at time $t = 0$, $H_{O_c} = 0$. Hence, it is zero at all time.

5 Control and Motion Planning

It seems that the most suitable system for movement of the robot is Fig. 5. Which consists of several processing cycles. In designing the diagram we have considered two assumptions: (1) We are able to construct the figure for driving the weights to the final condition, which will be discussed later, and (2) we have an algorithm which can calculate the next position of weights due to desired momentum for constructing the diagram. We, however, need two different kinds of motions, constant velocity, and constant acceleration.

5.1 Constant Acceleration. Traveling with constant acceleration implies that resultant momentum should have a constant value at each instance. Momentum is a superposition of two weights, momentum and friction of damping momentum elements, which friction momentum changes with velocity. Due to desired acceleration, we first calculate the momentum

$$m^w g \begin{bmatrix} -y_1 - y_2 - y_3 - y_4 \\ x_1 + x_2 + x_3 + x_4 \\ 0 \end{bmatrix} = \left[\sum_{n=1}^{4} (I_n^w + I_n^c + I_n^m) + I^s \right] \cdot \begin{bmatrix} \alpha_x \\ \alpha_y \\ \alpha_z \end{bmatrix}, \tag{8}$$

where α is acceleration and I is moment of inertia.

$$\text{Total Momentum (M)} = \text{Momentum caused by weights} + \text{Momentum caused by friction (velocity dependent)} \tag{9}$$

Due to Fig. 5, velocity is available so we can determine friction momentum in every instance. Therefore by Eq. (8), momentum caused by weights can be evaluated and then we can calculate the next position of the weights.

5.2 Constant Velocity. In this state, considering velocity, we can calculate friction momentum

$$\text{Total Momentum (M)} = \text{Momentum caused by weights} + \text{Momentum caused by friction} = 0. \tag{10}$$

Total momentum is equal to zero, as mentioned above, leading us to a constant weight momentum. This later momentum, however, changes with movement of the robot. Considered algorithm of calculation of momentum in each instance can help us to calculate the weights' positions during traveling.

5.3 Calculation of Velocity-Time Diagram. Area under the $\omega - t$ graph, Fig. 5, is equal to total displacement so, first we calculate the maximum momentum caused by robot and then we continue our calculation with a percentage of that number (because the robot cannot achieve that maximum momentum in every situation). By determining the acceleration rate and considering an optimum velocity for the robot, drawing the $\omega - t$ diagram is possible.

5.4 Trajectory Planning. In this section, we apply methods for steering the rolling robot. We suppose that the robot starts from rest, i.e., at time $t = 0$, $\omega_0 = 0$. Because of omnidirectional property of the robot, direct path is proposed and the traveling path is very close to the shortest path to the target.

The only parameter which defines the direction of movement is $\vec{M}$, [Eq. (4)]. Thus by distributing weights on the way, which leads the movement direction to the target, we can roll the robot to the desired point. The position of weights are subjected to the condition below:

$$\frac{-y_1-y_2-y_3-y_4}{y}=\frac{x_1+x_2+x_3+x_4}{x}, \tag{11}$$

where (x,y) is the target point. Notice that Eq. (11) has no dependence to z_i (z element of weights' positions). Here we introduce an algorithmic approach to distribute the weights as to satisfy the condition in Eq. (11).

Due to the discrete motion nature of the stepper motor, we have three statuses for each motor:

(i) off or steady state,
(ii) clockwise rotation, and
(iii) counterclockwise rotation,

where we mention them as 0, 1, and -1, respectively, so for our tetra-axis system, we have 81 different statuses for motors. Notice that the stepper motor cannot inverse the rotation direction instantly, so traverse from 1 to -1 is not allowed. Hence we should exclude that status leading such traverses, which will be discussed later. Now we develop an 81×4 matrix, *motor_movement*, which is all possible combinations of 0, 1, and -1 for four motors. As mentioned previously, we should neglect some status from our matrix. We do this by changing all four of one possible decision to zero.

When a motor is rotating it causes the respective weight, connected through the spoke, to move radially inside the sphere. Power screw rotates 1.8°, for each step of stepper motor, so it causes the weight to move d^w meters, as below:

$$d^w=\frac{l^s}{200}, \tag{12}$$

where l^s is the length of pitch on screws.

Due to Eq. (12), (x_n,y_n,z_n), and rotation direction of motor we can calculate the next position of weights as below:

$$x_{n-1}=\frac{d^w x_{n-0}}{\sqrt{x_{n-0}^2+y_{n-0}^2+z_{n-0}^2}}+x_{n-0}, \tag{13}$$

$$y_{n-1}=\frac{d^w y_{n-0}}{\sqrt{x_{n-0}^2+y_{n-0}^2+z_{n-0}^2}}+y_{n-0}. \tag{14}$$

With *motor_movement* matrix [Eqs. (13) and (14)] we develop an $8.1\times4\times2$ matrix, *weight position*, of all possible positions of weights. Then we calculate two independent matrices A and B with 81 components per, members are $(x_1+x_2+x_3+x_4)/x$ and $-(y_1+y_2+y_3+y_4)/y$, respectively, and sort A and B with an algorithm like merge sort or quick sort, which their orders being $n\log n$. Then we use a selection algorithm to choose the best solution for our motor's movement. The pseudocode of selection part of our selection algorithm is as below:

```
j←1
for i←[1 . . . 81]
    if [B(i)<A(j)] and [B(i+1)>A(j)] then
        C(j)←i
        j←j+1
min←0
for i←[1 . . . j]
    if {A(i)−B[C(i)]<A(min)−B[C(min)]} then
        min←i
    if {A(i+1)−B[C(i+1)]<A{min−B[C(min]} then,
        min←i
```

where min refers to the index of the best solution in *motor_movement*.

The analytical model, Sec. 4, and control strategy, Sec. 5, are used for steering the robot from the beginning to destination. Trajectory planning, Sec. 5.5, is used for evaluating the motors' status and by the use of analytical model, where we can define robot, weight positions, and angular velocity.

Algorithm, discussed above, is used for finding the best status of motors, which fits Eq. (11). Due to the discrete nature of motors, the exact calculation of Eq. (11) is not possible, so the closest equality is selected. This is the point that causes a small vibration on velocity and position of the robot, which will be shown in the next section.

Table 1 The experimental setup configuration

Variable	Quantity	Unit
Holding torque of motors	3.250	kg/cm
Weight of motor (each)	0.570	kg
Length of spokes	0.160	m
Radius of spokes	0.040	m
Pitch of power screw	0.060	m
Weight of power screw (each)	0.650	kg
Weight of unbalanced masses (each)	1.125	kg
Radius of spherical shell	0.290	m
Weight of spherical shell	2.750	kg

6 Experimental Results

In this section, the validity of the model is validated by comparing trajectories found by experiment with those predicted by integrating the model for a series of setups. The calculations are done by a low-order numerical calculator in MATLAB 6 using a time step of 0.01 s. The experimental setup has the configuration presented in Table 1.

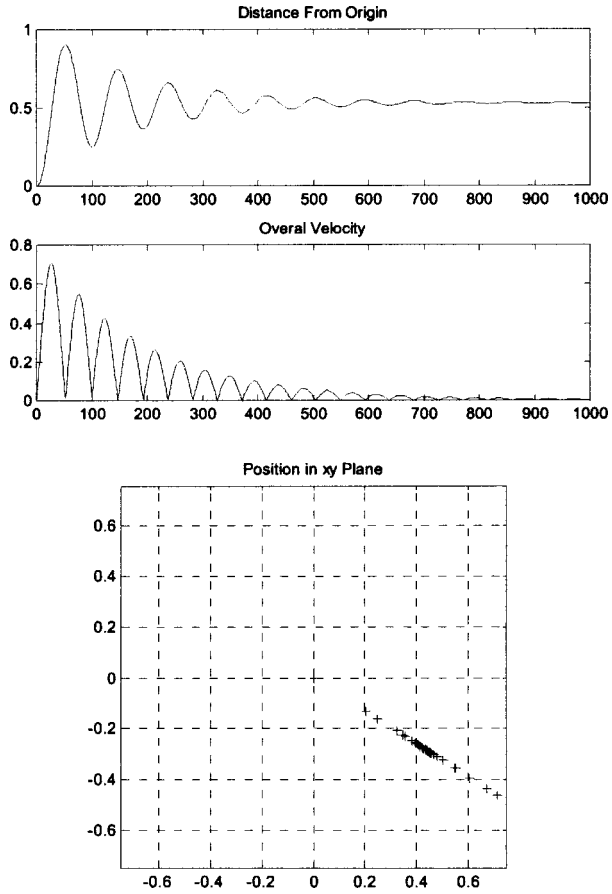

Fig. 6 Experience discussed in Sec. 6 1

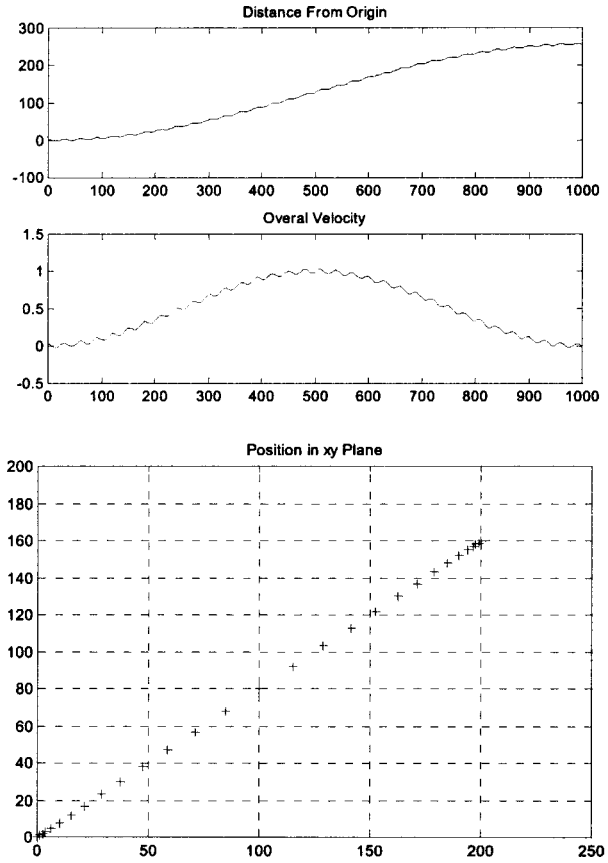

Fig. 7 Experience discussed in Sec. 6 2

For several missions, the experimental results agree well with those of the model. In each case, the experimental trajectory follows the predicted one within a reasonable accuracy. Some factors that contribute to these inaccuracies are:

(i) the center of mass of the robot is not exactly at the geometric center of the robot;

(ii) imperfections on the surface of the sphere; and

(iii) open-loop nature of the robot control.

The following are several issues of experimental results. The figures are in three parts; figure in the top-left shows the distance of the robot's center from origin, which the robot has began its travel, figure in bottom-left shows the absolute velocity and figure on the right shows the movement of robot in xy plane, predicted by dynamic model.

6.1 Unstable Robot With Fixed Weights. In this setup, we placed the robot so that one of the spokes lay on the z axis, perpendicular to the moving surface, and one of the other spokes lay on yz plane. Weights are distributed in 26, 31, 24, and 18 cm far from center of the robot on the spokes and the motors are kept steady. The robot will proceed to place it's center of the mass in the perpendicular direction of it's center. The results are illustrated in Fig. 6.

6.2 Unsteady Weights and Fixed Destination. Robot begins its mission at (0,0) and the destination point is at (160,240) cm. Direct path is chosen and the robot distributes weights in a sense that it will reach the target point on the shortest possible path. Results are shown in Fig. 7.

7 Conclusion

An autonomous omnidirectional spherical rolling robot was designed and built. A mathematical model of the robot motion was developed using the no-slip rolling constraint and conservation of angular momentum, and an algorithmic motion planning was developed. The model was validated through a set of experiments. Simulation and experimental trajectories of the robot on the plane were found to agree to a reasonable accuracy. Trajectories are quite accurate despite lack of on-board feedback control. As compared to existing motion planners, most of which require intensive numerical computation, our strategy involve simple algorithmic iteration and provide the scope for easy implementation. This study demonstrates the feasibility of the idea and it is expected to be improved in the future.

Appendix

Here it is shown how the angles between the spokes are 109.47°. The tetrahedral configuration is shown in Fig. 8. O is the center of the robot, and OA, OB, OC, and OD are the four spokes on which the weights are distributed along. The point O' is the projection point of O on ABC plane. Points A', B', and C' are the center points of BC, AC, and AB, respectively. The length of each spoke is supposed to be one unit.

$$OD = OA = OB = OC = 1, \tag{15}$$

In ΔAOB:

$$OC' \perp AB, \tag{16}$$

and ΔAOB is an equilateral triangle, so

$$AC' = \alpha/2, \tag{17}$$

where α is the length AB.

In $\Delta CC'A$, which is a right-angled triangle,

$$CC' = \sqrt{\alpha^2 - \frac{\alpha^2}{4}}, \tag{18}$$

$$CC' = \frac{\sqrt{3}}{2}\alpha, \tag{19}$$

so

$$O'C' = \frac{\sqrt{3}}{6}\alpha, \tag{20}$$

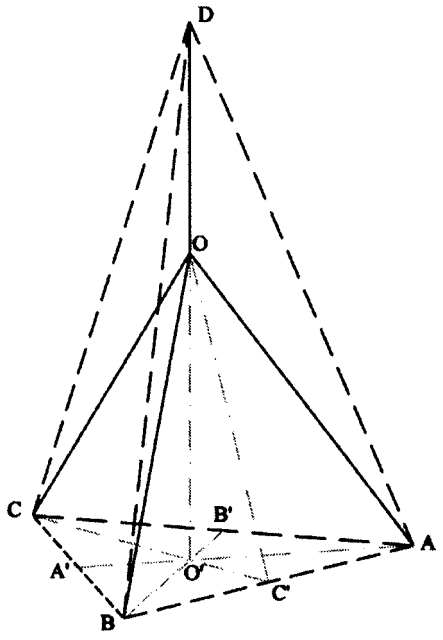

Fig. 8 The tetrahedral configuration: The spokes are shown as OA, OB, OC, and OD

$$O'A = \frac{\sqrt{3}}{3}\alpha. \tag{21}$$

In a right-angled triangle $\Delta O'AD$:

$$O'D^2 + O'A^2 = AD^2, \tag{22}$$

$$(1 + O'O)^2 + (1/3)\alpha^2 = \alpha^2, \tag{23}$$

$$O'O = \sqrt{\frac{2}{3}}\alpha - 1. \tag{24}$$

From the system of equations following:

$$\begin{aligned} &\text{in } \Delta OO'C': O'C'^2 + O'O^2 = OC'^2 \\ &\text{in } \Delta OC'A: OC'^2 + AC'^2 = OA^2, \end{aligned} \tag{25}$$

$$\left(\frac{\sqrt{3}}{6}\alpha\right)^2 + \left(\sqrt{\frac{2}{3}}\alpha - 1\right)^2 = OC'^2 \tag{26}$$

$$OC'^2 + (\alpha/2)^2 = 1$$

we can obtain α as

$$\alpha = \frac{2}{3}\sqrt{6}, \tag{27}$$

and in a right-angled triangle $\Delta OC'A$:

$$\sin\angle AOC' = AC'/OA, \tag{28}$$

$$\sin\angle AOC' = \alpha/2, \tag{29}$$

so

$$\angle AOC' = \sin^{-1}\frac{\sqrt{6}}{3}, \tag{30}$$

and the angle $\angle AOB$ will become

$$\angle AOB = 2\sin^{-1}\frac{\sqrt{6}}{3}, \tag{31}$$

which is 109.47°.

Acknowledgments

The support of the Azad University of Qazvin is gratefully acknowledged. Thanks are also due Dr. Moosakhani and Dr. Gharagoozloo for their support and encouragement, and M. Chitsazan and A. Delnavaz for their help on building the robot.

References

[1] Masayoshi, W., and Shunji, M., 1996, "Modeling and Control of a New Type of Omnidirectional Holonomic Vehicle," in AMC'96, pp. 265–270.

[2] Ferriere, L., Raucent, B., and Campion, G., 1996, "Design of Omnimobile Robot Wheels," in *Proceedings of IEEE International Conference on Robotics and Automation*, pp. 3664–3670.

[3] Tang, J., Watanabe, K., and Shiraishi, Y., 1996, "Design and Traveling Experiment of an Omnidirectional Holonomic Mobile Robot," in *Proc. IEEE Int. Conf. Intelligent Robots and Sys.*, pp. 66–73.

[4] Agrachev, A. A., 1999, "An Intrinsic Approach to the Control of Rolling Bodies," in *Proceedings of the Conference on Decision and Control*, pp. 431–435.

[5] Halme, S., Schonberg, T., and Wang, Y., 1996, "Motion Control of a Spherical Mobile Robot," in *Proceedings of AMC'96*, pp. 259–264.

[6] Bicchi, A., Balluchi, A., Prattichizzo, D., and Gorelli, A., 1997, "Introducing the Sphericle: An Experimental Testbed for Research and Teaching in Nonholonomy," in *Proc. IEEE Int. Conf. on Robotics and Automation*.

[7] Bhattacharya, S., and Agrawal, S. K., 2000, "Spherical Rolling Robot: A Design and Motion Planning Studies," in *Proceedings of IEEE International Conference on Robotics and Automation*.

[8] Mukherjee, R., Minor, M. A., and Pukrushpan, J. T., 1999, "Simple Motion Planning Strategies for Spherobot: A Spherical Mobile Robot," in *Proceedings IEEE International Conference on Decision and Control*, pp. 2132–2137.

[9] Ferriere, L., and Raucent, B., 1998, "RollMOBS, A New Universal Wheel Concept," in *Proceedings of IEEE International Conference on Robotics and Automation*, pp. 1877–1882.

[10] Roberson, R., and Schwertassek, R., 1988, *Dynamics of Multibody Systems*, Springer, New York.